Journal of Materials Chemistry A

Accepted Manuscript

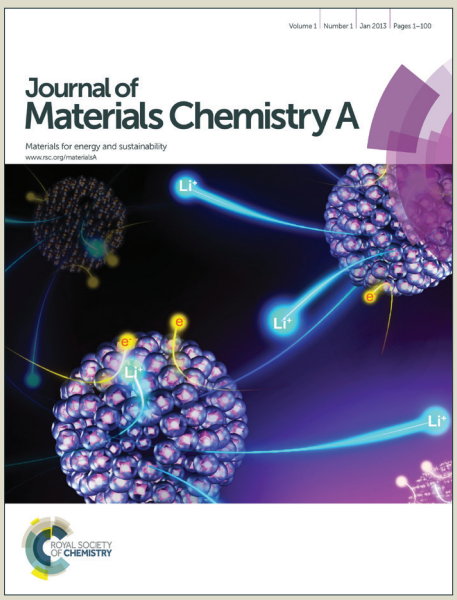

ROYAL SOCIETY OF CHEMISTRY

www.rsc.org/materialsA

Journal of Materials Chemistry

ARTICLE

Facile Method for Preparation of Self-Healing Epoxy Composites: Using Electrospun Nanofibers as Microchannels

Received 00th January 20xx,
Accepted 00th January 20xx

DOI: 10.1039/x0xx00000x

www.rsc.org/

Vahdat Vahedi,[a] Pooria Pasbakhsh,[a]* Chai Siang Piao[b] and, Chan Eng Seng[b]

Abstract: Electrospun nanofibrous mats of polyacrylonitrile (PAN) carrying epoxy and amine dual healing solutions were incorporated into epoxy matrix to impart self-healing functionality. The self-healing performance of the epoxy composites was measured using fracture toughness tests. The average healing efficiency was approximately 75% at 50 °C and 38% at room temperature. The epoxy composites were capable of repeated self-healing for up to 6 times at room temperature. This new method of preparing self-healing epoxy is cheap and versatile and can be optimized for mass production of high performance self-healing structural composites.

Introduction

Inspired by biological systems, the preparation of materials that are able to repair themselves without external intervention has been a matter of intense research in the past decade. One of the effective strategies developed for making self-healing materials, namely extrinsic self-healing, involves incorporation of healing agents inside a polymeric matrix. The healing agents can be released into crack spaces after damage and trigger the healing process. The main challenge of this strategy is to find a suitable carrier system to incorporate the healing agents inside the polymeric matrix. Ideally, a carrier system should be strong enough to withstand the mechanical stresses during the manufacturing processes (such as mixing, curing and etc.) without releasing the healing agents. On the other hand, this carrier system should break during propagation of cracks inside the matrix and release adequate amount of active healing agents into the crack planes to heal the damage.

White et al. prepared an autonomous self-healing polymer by using microcapsules loaded with liquid healing agent (dicyclopentadiene (DCPD)) and a solid-phase catalyst (Grubbs catalyst) into the epoxy matrix. The microcapsules were prepared by in situ polymerization of urea-formaldehyde (UF) at the interphase of emulsified DCPD in water [1]. Thereafter, numerous studies have been conducted to enhance the self-healing performance of microencapsulated systems by studying the effects of different healing agents [2-6], the size [7-9] and strength [10-12] of microcapsules to restore mechanical properties, electrical conductivity, or corrosion resistance in corresponding self-healing composites. Cho et al. [13, 14] used a system containing phase-separated droplets of healing agent (siloxane-based materials) without encapsulation to impart self-healing functionality in epoxy and vinyl ester resins. Recently, Zhang et al. utilized hollow glass bubbles to carry healing chemicals inside the epoxy matrix [15-17]. They made through-holes at the micron level in the shell of glass bubbles by etching them with dilute hydrofluoric acid (HF) using a specially designed mixer [18]. The healing agents were infiltrated into the etched GBs using a vacuum assisted device [18]. The major drawbacks of a capsule-based self-healing system can be listed as a complicated microcapsule preparation methods (high number of involved chemicals and processing parameters), problems in processing of microcapsules (possible breakage of microcapsules and their poor distribution in the composite), and the depletion of healing agents after the first healing.

In another approach, continuous hollow fibers (tubes) was used to incorporate the healing agents inside the polymeric matrix [19-22]. The first polymer-based self-repair material by hollow fibers concept was prepared by Dry et al. [19, 20] using glass pipettes of millimetre-diameter. Motuku et al. [21] showed that the type and the diameter of hollow fibers, their concentration and spatial distribution as well as the thickness of the specimen could have critical influence on the healing efficiency. Bleay et al. [22] used small diameter (i.e. 15 µm external and 5 µm internal diameter) hollow glass fibers to reduce the detrimental effects (reduction in the initial strength) of hollow fibers in epoxy matrix. Bond and coworkers further developed this system, using in house made hollow glass fiber in carbon and glass fiber reinforced composites with self-healing and damage sensing properties [23-27]. The difficulties in production of hollow fiber with consistent hollowness and concentricity [28], the adverse effect of fiber on mechanical properties in the case of large-diameter fibers [21, 22], the problems in loading healing agent in small-diameter fibers

[a] Mechanical Engineering Discipline, School of Engineering, Monash University Malaysia, Jalan Lagoon Selatan, Bandar Sunway, 47500, Selangor, Malaysia.
[b] Chemical Engineering Discipline, School of Engineering, Monash University Malaysia, Jalan Lagoon Selatan, Bandar Sunway, 47500, Selangor, Malaysia.
Email: Pooria.Pasbakhsh@monash.edu

(especially for healing agents like cyanoacrylate or viscous epoxy) [22] are among the challenges of this approach.

In addition, the abovementioned carrier systems (hollow fiber and microcapsules) were unable to heal the same location of the material repeatedly (more than once) due to the depletion of healing agents or blockage of the tubes openings. To address this problem, a microvascular system consisting of a series of interconnected channels located within a polymer matrix was developed to provide higher reliability with regard to channel blockages and a larger accessible reservoir for the healing agent(s) [29-32]. To produce the interconnected vascular network, first a sacrificial scaffold with specially formulated ink was made by direct-ink writing technique. This scaffold was then infiltrated with uncured resin. After solidification of the resin, the ink was removed by applying heat and light vacuum leaving a hollow network inside the polymer resin [33]. By optimizing the healing chemistry and geometry of vascular channel network, a healing efficiency of 50% was achieved even after 30 cycles of healing [29, 31, 34]. Trask and Williams developed a vascularized system for self-healing sandwich panels and composite laminates. They used PVC straight tubes and drilled a hole through the core and into the tubes at appropriate locations to form a network [35-37]. Esser-Kahn et al. [38] made a microvascular template in fiber-reinforced composites through weaving of sacrificial catalyst-impregnated polylactide (PLA) fibers into 3D woven glass preforms and subsequent removal of sacrificial fiber by heating. These microchannels can act as stress concentrators causing premature failure in the structure. Olugebefola et al. used an electrostatic layer-by-layer assembly technique to incorporate halloysite nanotubes as reinforcement at microvascular channels surfaces to improve the mechanical properties of microvascular structure [39].

Advancements in electrospinning process provided a simple and versatile method for producing non-woven fibrous mats of nano- to micron-sized fibers with extremely high surface-to-volume ratio [40, 41]. In the recent years, the special ability of electrospun matrixes to load and sustained release of chemicals has attracted tremendous research interest to develop tailored drug delivery systems based on electrospun mats [40, 41]. Making core/shell nanofibers through coaxial or emulsion electrospinning is one of the techniques that have been developed for loading chemicals such as drugs in electrospun mats. Exploiting this concept, Park et al. [42] separately encapsulated two parts of polysiloxane healing system in electrospun polyvinylpyrrolidone (PVP) nanofibers with bead-on-string morphology and used the coaxial electrospum mats to add self-healing functionality to polyurethane based coating.

Another technique for loading chemicals in electrospun mats is by post-spinning loading where chemicals are loaded to the pores of as-electrospun mat [40, 41]. This method has the benefits of simple loading process, higher loading capacity, no exposure of chemicals to electrospinning process, and higher release rate. These characteristics make this method especially suitable for self-healing of structural composites; however the possibility of using as-electrospun membrane to make self-healing composites has not been studied yet. In this work, we have prepared porous electrospun PAN scaffold to incorporate the healing agents (dual amine–epoxy system) inside epoxy matrix and demonstrated the effectiveness of this new method for production of self-healing structural composites. PAN is comparatively easy to be electrospun and the properties of PAN electrospun mats can be altered through manipulating the electrospinning conditions or heat treatment after the electrospinning. The advantages of this system over previously reported self-healing systems (such as capsules-based or hollow fibers systems) is that the electrospinning is a simple, cheap and high throughput process. The loading of healing agents into micropores of electrospun mat is much easier compared to hollow fibers and this method can be easily used to carry reactive healants, as healing agents are not exposed to encapsulation or electrospinning process.

Experimental

Materials:

Polyacrylonitrile (PAN) with molecular weight of 150,000 g/mol and N,N-Dimethylformamide (DMF) solvents from Sigma-Aldrich were used for electrospinning. Medium viscosity bisphenol A epoxy resin (Epikote 828, Momentive) with epoxide equivalent weight (EEW) of 185–192 g/eq were used as the base resin. Low viscosity bisphenol A epoxy resin (Araldite 506, Sigma-Aldrich) with EEW of 172–185 g/eq diluted with 30 wt% neophentyl glycol diglycidyl ether (NGDGE, Sigma-Aldrich) as the reactive diluents was used as epoxy healing agent. NGDGE was used to reduce the viscosity of epoxy for better flowability as reported by Zhang et al. [15-17]. Diethylenetriamine (DETA) from BASF was used as curing agent to cure the base epoxy matrix as well as latent amine curing agents for self-healing.

Preparation of electrospun mat:

Homogenous solution of 8 wt.% PAN in DMF was prepared by stirring at room temperature for 24 h. The PAN solution was added to a horizontally-aligned syringe with 1 mm diameter metallic needle and was fed at a constant rate of 1.5 ml/min using a syringe pump (NE-1000, New Era Pump Systems Inc.). An electrode was fixed to the needle and connected to the high voltage power supply. A rotating drum was connected to the ground electrode and used as collector. The distance and voltage difference between needle and collector were set to 20 cm and 14 kV, respectively. Two hours of electrospinning were performed to obtain a 200-300 µm thick electrospun non-woven mat.

Loading of healing agents:

The electrospun mat was cut into small strips (2 cm length and 1-2 mm width). The strips were easily loaded with healing agents by separately immersing them in the liquid epoxy solution or DETA. The loaded strips were separated from the solution and hanged for 30 min to remove the extra epoxy or DETA.

Preparation of self-healing composites:

Tapered double-cantilever beam (TDCB) geometry with a long moulded groove of 60 mm were used to evaluate the self-

healing ability of the composites, as it was suggested to be the best geometry to quantify the healing efficiency of different self-healing materials due to its less dependency to the crack length [43]. The neat epoxy samples were prepared by mixing 100 parts Epikote 828 epoxy with 12 parts curing agent DETA. The mixture was then degassed for 30 min, poured into a stainless steel mold, and cured for 24 h at room temperature. The same procedure was used to prepare self-healing samples, while the PAN electrospun stripes loaded with epoxy or DETA were alternatively layered up across the pre-moulded groove (**Figure 2**) during casting of epoxy mixture. The fraction of DETA/epoxy loaded strips was 1/1. The loaded strips did not touch each other during and after manufacture and epoxy matrix filled the spaces between the strips as illustrated in **Figure 3**-a.

Characterization:

Evaluation of healing efficiency: The self-healing properties of epoxy/PAN composites were studied by measurement the compact tension fracture toughness of TDCB samples (**Figure 1**). A pre-crack was made by gentle tapping of a sharp razor blade into the molded groove of a TDCB specimen. The specimens were then loaded by Intron universal testing machine at 1 mm/min speed to the complete fracture of the specimens along the pre-molded groove. Then the crack faces were rejoined together to be self-healed at specified temperature for a certain period of time (72 hr). The healed samples were tested again following the above procedure. The healing efficiency, η, is defined as the ratio of fracture toughness of healed materials, K_{IC}^{Healed}, to that of virgin ones, K_{IC}^{Virgin}:

$$\eta = \frac{K_{IC}^{Healed}}{K_{IC}^{Virgin}} = \frac{P_{C}^{Healed}}{P_{C}^{Virgin}}$$

Tensile modulus and tensile strength of nanocomposite were determined according to ISO 527-1 on a universal testing machine (Instron 3366). Dumbbell shape samples in conformance to Type I of ISO 527-1 were prepared by the same method and the same distribution of strips as described above. The samples were pulled by pneumatic grips at a crosshead speed of 1.0 mm/min to obtain stress-strain curve of samples.

Microscopic observations: The electrospun PAN strips and the fractured surface of the composites were studied using HITACHI SU8010 field-emission scanning electron microscope (FE-SEM). To prepare the specimens for FE-SEM analysis, samples were coated with platinum using QUORUM-Q150RS sputter coater and transferred into FE-SEM for imaging. Optical microscopic images of the fractured surfaces of composites were captured by using an Olympus BX41 microscope.

Porosity measurement: The size of nanofibers and the pores formed between the fibres was measured on FE-SEM micrographs using ImageJ software (ImageJ software 1.48v, National Institutes of Health, USA), as described in [1-3]. The percentage of the fibre area relative to the total section surface area in each image was defined as the present porosity.

Results and discussion

Figure 2 shows the field-emission scanning electron microscopy (FE-SEM) of the PAN fibrous mats produced by electrospinning. PAN has a good ability to electrospin and provides fibers with rough surface (see **Figure 2**-c) which may increase their interaction with epoxy matrix. The diameter of nanofibers was in the range of 300 to 550 nm and their average diameter was 430 nm. The fibers are densely packed in a three-dimensional manner providing a porous scaffold

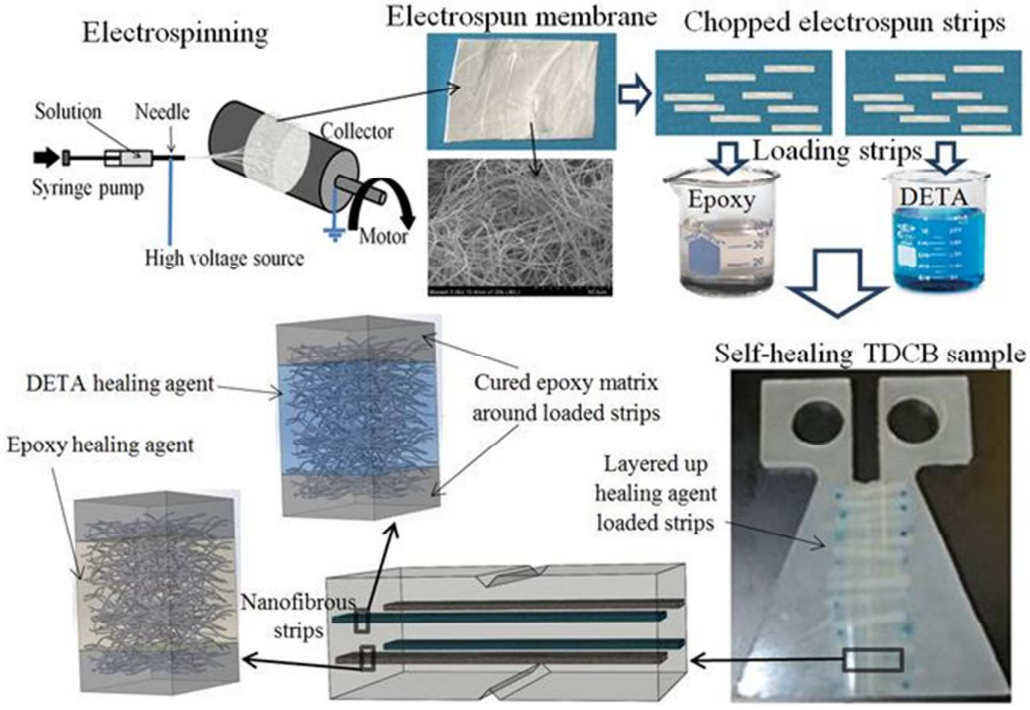

Figure 1: Schematic illustration of preparation method, structure of self-healing specimen using electrospun membrane.

which can be used for loading and accommodating chemicals such as epoxy and DETA healing agents. The size of pore formed between nanofibers was in the range of 0.2-10 µm with the measured porosity of ca. 70-80%. The morphology of electrospun fibers and pore size of the electrospun mat can be further optimized by adjusting electrospinning parameters (including polymer characteristics (molecular weight, molecular-weight distribution and architecture), solution properties (viscosity, conductivity, concentration and surface tension), electric potential, flow rate, distance between the needle and collection screen, ambient parameters (temperature, humidity and air velocity in the chamber), motion and size of the collector and needle gauge) to improve the loading and release properties of the electrospun mats [40].

The preparation method and the structure of self-healing specimen are illustrated in **Figure 1**. Electrospun strips are used to load and incorporate healing chemicals inside the epoxy matrix. Each nanofibrous strip weighs between 0.0020 and 0.0027 g and each strip can accommodate 0.0090-0.0150 g of healing agents. The porous structure of electrospun strips impedes abrupt release of healing agents and keeps them inside the strips during formation of the composite. After processing and curing of the epoxy, a solid matrix is formed around the nanofibers, which prevent release of the healing chemicals into the virgin composites. The diffusion of healing agent into epoxy matrix was traced by the microscopic observation of the fractured surface while a red dye was added to the healing agent for visualization (**Figure 3**-b). The epoxy matrix could partially infiltrate into the walls of strips (10-15 µm, **Figure 3**-b section II) that resulted in good interaction between epoxy matrix and nanofibrous strips (see also **Figure 8**-d and e). Tuning the properties of electrospun mat (their porosity, fibre diameter, pore size, and etc.) plays an important role in the successful preparation of self-healing composites by this method. In case of electrospun mats with wrong properties, leakage and diffusion healing agents out of the nanofibers interfered the curing of the epoxy matrix. This resulted in poor interactions between the strips and epoxy matrix and pull out of the strip during the mechanical tests.

Figure 4 illustrates the self-healing mechanism of epoxy matrix using electrospun nanofibrous mats containing self-healing agents. When a crack is formed inside the matrix, the healing agents (epoxy and DETA) will be released into the crack planes and form films of cured healing agent at the interface of the cracks which bonds the crack surfaces together. This method is comparable to hollow fiber systems but the preparation and loading of electrospun mat is much easier and more cost effective than hollow fibers and the geometry of the electrospun strips can be varied according to possible spatial requirement in the composite products.

A typical load-displacement curve of a self-healing composite sample is shown in **Figure 5** demonstrating a recovery of approximately 75% relative to the fracture load of virgin sample. In contrast, neat epoxy samples showed no healing and the broken pieces could not be bonded together. The addition of loaded nanofibrous strips did not decrease the inherent toughness of the epoxy. From the fracture toughness tests, the average critical load for virgin self-healing samples containing the strips (85 N) was 15% higher than the average value of the neat epoxy samples (75 N), indicating a slight increase in the fracture toughness of epoxy.

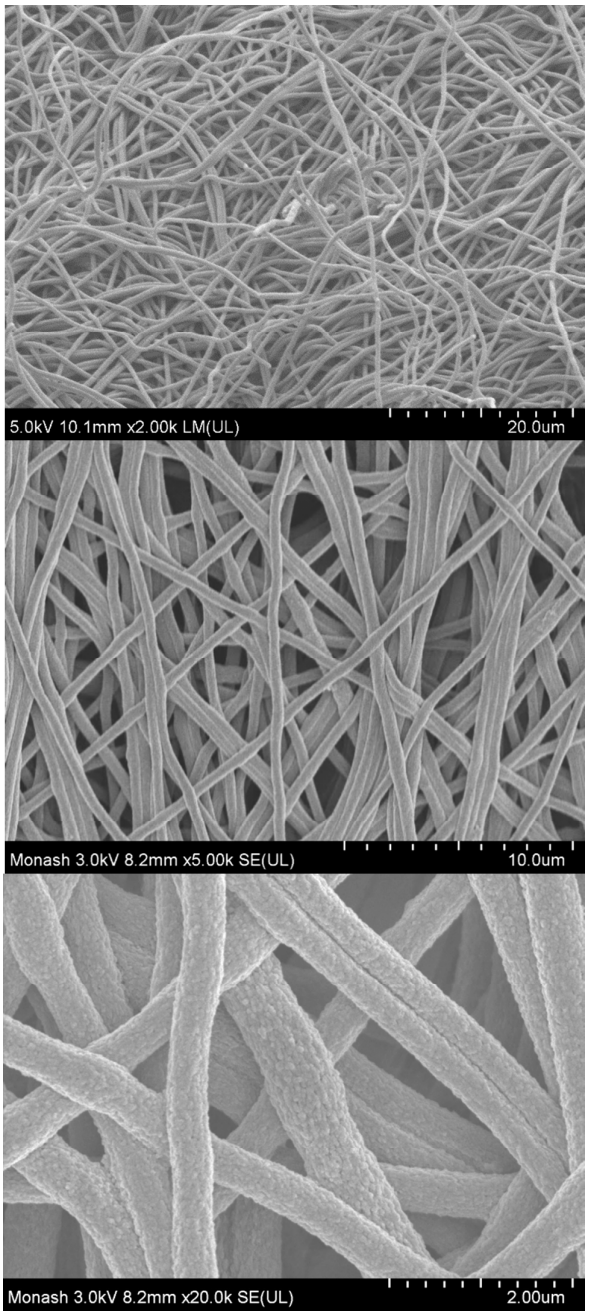

Figure 2: FE-SEM images of nonwoven electrospun fibres mats at different magnifications.

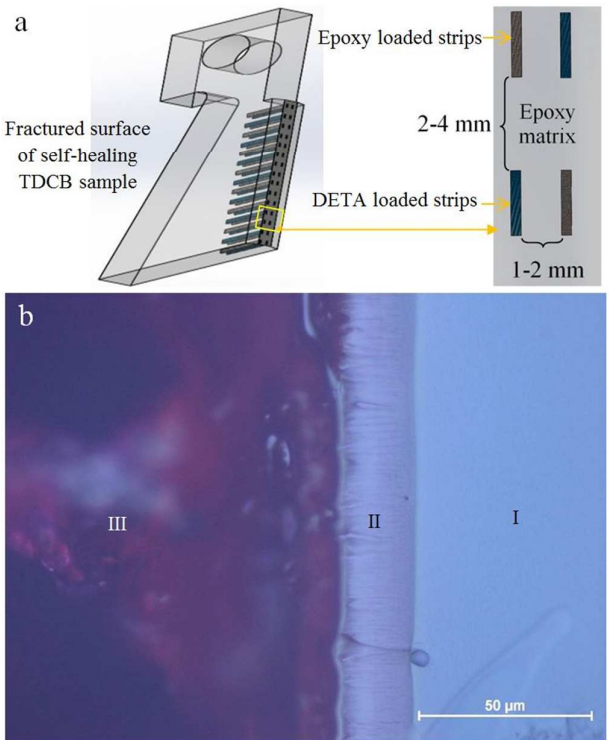

Figure 3: a) Schematic illustration of the fractured surface and spatial distribution of strips, b) tracing the release of healing agents from strips during preparation: I) epoxy matrix**,** II) diffused epoxy matrix in strips wall, III) healing agent loaded strip (red dye was added for visualization).

A set of five independently prepared self-healing composite samples showed an average healing efficiency of 70% at 50 °C

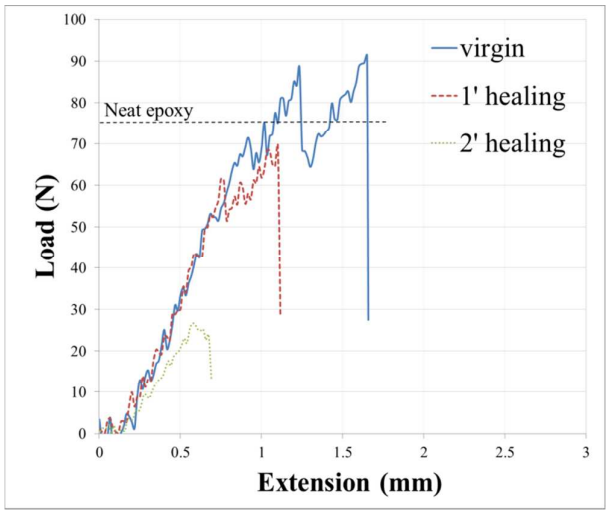

Figure 5: Typical load-displacement curves of virgin and healed specimen at 50 °C.

(**Figure 6**-a). The samples healed at 50 °C, demonstrated self-healing ability after second fracture; however the second healing percentage (22%) was much lower than the first one. For these samples no healing was observed in third healing cycle. The reduction of self-healing in these samples is mainly attributed to the deactivation of DETA part of healing system, as the release of epoxy healing agent could be still observed at the crack surfaces (**Figure 7**-c and d) and discoloration of DETA loaded strips was obvious (DETA strips turned to brownish colour, **Figure 7**-e). The reduction in healing efficiency of dual DETA-epoxy system upon exposure to heat was reported in previous studies [5, 44].

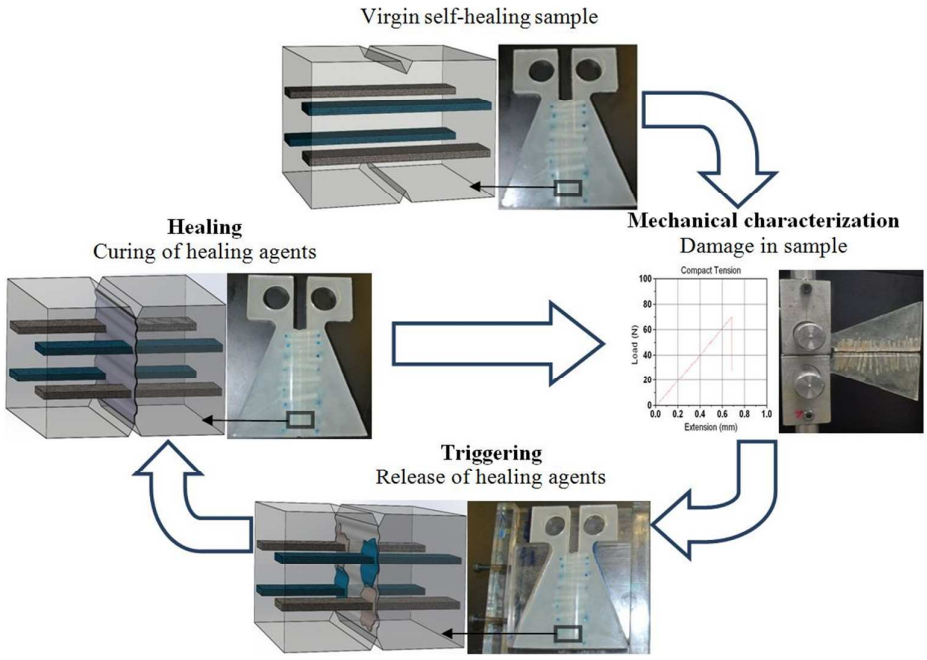

Figure 4: Schematic diagram of self-healing process.

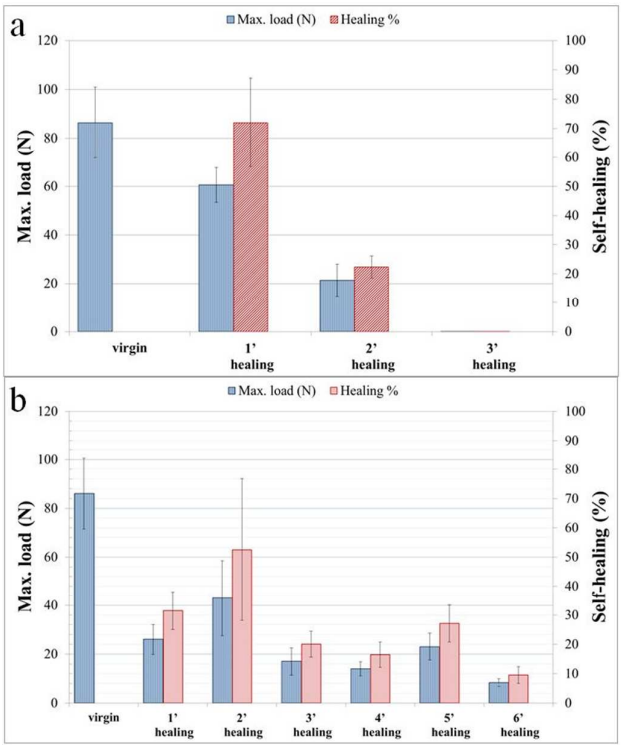

Figure 6: Healing efficiency at a) 50 °C b) at room temperature.

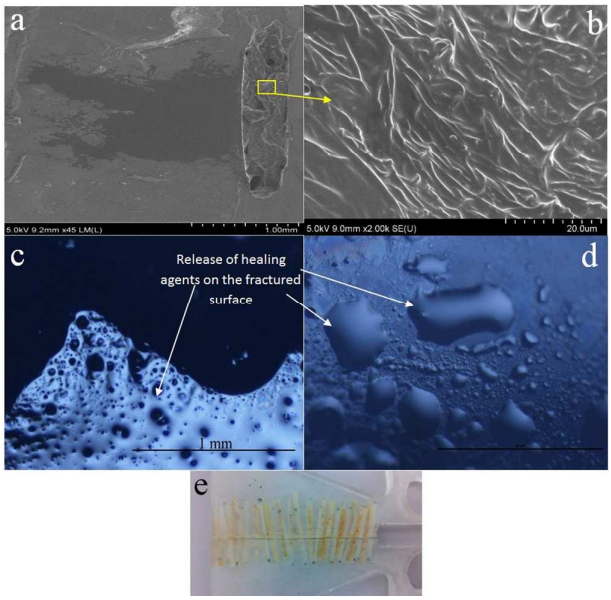

Figure 7: a) and b) FE-SEM micrograph of fractured surface after first breakage (before healing) showing the entrapment of healing agents inside nanofibrous strips, c) and d) Optical microscopic images showing the release of liquid epoxy to fracture surface after 2 times healing at 50 °C, e) discoloration of DETA-loaded strips.

Figure 6-b shows the healing efficiency of samples that were healed at room temperature. The healing efficiency of the composites at room temperature (38%) decreased considerably compared to the healing at 50 °C (75%), however, the samples healed at room temperature demonstrated the ability for repeated healing up to 6 times. The healing efficiency at room temperature was in the same range as the healing efficiency reported by Zhang and Yang,[17] where hollow glass bubbles were used as carrier of healing epoxy-amine system. The decrease in the healing efficiency at lower temperature could be attributed to the lower reaction rate between the epoxy and the hardener, slower evaporation of the solvent (NGDGE), slower diffusion rate of epoxy and DETA healing agents thus impeding the mixing between the two. The ratio of amine to epoxy is another important factor that affects the self-healing performance of dual epoxy-amine healing chemistry (both at room and high temperature). Previous studies on dual epoxy-amine healing chemistry showed that the variation of the ratio of amine to epoxy could cause up to 60% change in the healing efficiency of the system.[6, 15, 17] In this method, the amount of healing agent can be controlled by the amount and the spatial distribution of nanofibrous strips. Therefore, optimization of the amount and the spatial distribution of amine and epoxy loaded nanofibrous strips or using other healing agents in electrospun nanofibrous carrier system may further increase the self-healing efficiency of the composites with the benefit of repeated healing.

The FE-SEM micrographs of the fractured surface of the composites right after the first fracture (before healing) are shown in **Figure 7**-a and b. The magnified view of the electrospun strips shows that the nanofibers are surrounded by healing agents revealing the ability of nanofibrous strips to embed and carry the healing agents. After fracture of the

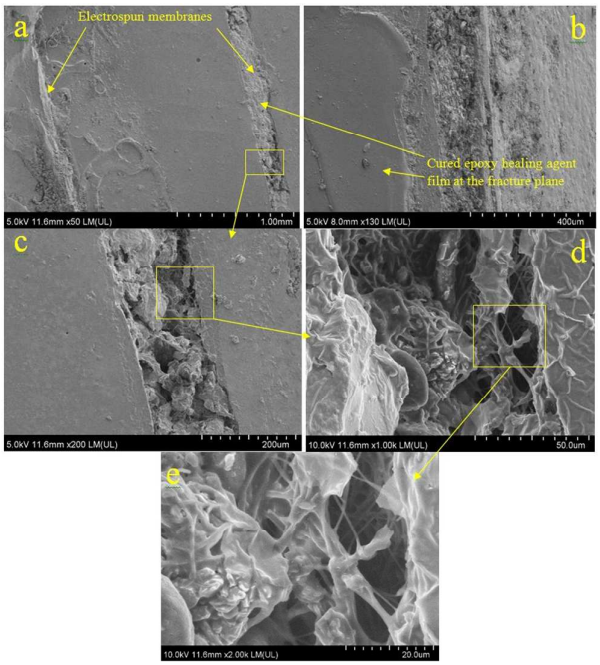

Figure 8: a) two adjacent electrospun strips, b) the cured healing agent films covering parts of the fracture surface, c) and d) closer view of the electrospun membrane

composites, the healing agents could be released to the fractured surface and trigger the healing process. The release of healing chemicals could be observed on the fractured surface of composites, even after a few cycles of healing (**Figure 7**-c and d).

The FE-SEM micrographs of the fractured surfaces of composites after the first healing are shown in **Figure 8**. The cured healing agent films are obvious on some parts of the fracture surface (**Figure 8**-a) as well as on top of the electrospun strips (**Figure 8**-b). The remaining parts of cured healing agent films were placed on the other side of the fractured surface. The release and depletion of healing agents from nanofibrous strips can be deduced by comparing the micrographs that showed the fractured surface before and after healing (see **Figure 7**-b and **Figure 8**-d). Closer examination of the electrospun strips generally show good interactions between the strips and epoxy matrix (**Figure 8**-d and e). The epoxy matrix could infiltrate the walls of the electrospun strips. In microcapsules- and hollow tubes-based healing systems, the cracks have to break the container shells to release the healing agents and trigger the healing process. Unlike the microcapsules and hollow tubes, the healing agents in this method are not embedded inside rigid solid shells and the propagating cracks do not need to break the container shells to release the healing agent. This work introduces the self-healing materials based on microporous carrier without external solid shell.

The effect of the loaded membranes on the tensile properties of the epoxy is shown in **Figure 9**. Incorporation of loaded strips did not have noticeable effect on the modulus of the epoxy. However, the tensile strength of epoxy decreased by 18% after incorporation of loaded strips, which can be attributed to the stress concentration at the strips. The adverse effect on mechanical performance of neat epoxy is one of the drawbacks of self-healing methods. Similar to all fiber composites, the mechanical behaviour as well as self-healing performance of the composites prepared by this method is highly dependent on the amount and distribution of nanofibrous strips and this can be optimized to achieve the best balance of self-healing and mechanical performance.

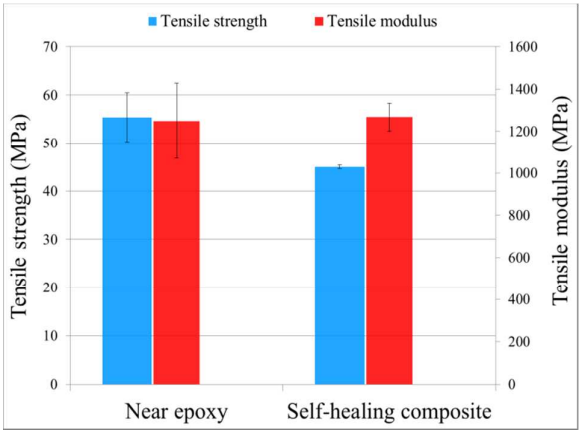

Figure 9: Effect of loaded strips on tensile properties of epoxy.

Conclusions

PAN electrospun nanofibrous mat was successfully used as carrier of healing agents to prepare self-healing epoxy composite with high self-healing efficiency for repeated times (6 times at room temperature). Compared to other carrier systems this system offers a number of benefits: it is a cost effective, versatile and high throughput process; the loading of healing agents is straightforward; and there is more chemical compatibility with various matrixes and healing agents; it is possible to spatially vary the location and concentration of healing chemicals. The self-healing efficiency of this system can be further improved in terms of healing agent chemistry and nanofibers properties for production of high performance self-healing structural composites.

Acknowledgements

Financial support from Monash University Malaysia is gratefully acknowledged for the PhD scholarship scheme. This project was funded by a grant FRGS/2/2013/TK04/MUSM/03/1 from the Ministry of Higher Education, Malaysia.

Notes and references

1. S. R. White, N. R. Sottos, P. H. Geubelle, J. S. Moore, M. R. Kessler, S. R. Sriram, E. N. Brown and S. Viswanathan, *Nature*, 2001, **409**, 794-797.
2. J. M. Kamphaus, J. D. Rule, J. S. Moore, N. R. Sottos and S. R. White, *Journal of The Royal Society Interface*, 2008, **5**, 95-103.
3. G. O. Wilson, M. M. Caruso, N. T. Reimer, S. R. White, N. R. Sottos and J. S. Moore, *Chemistry of Materials*, 2008, **20**, 3288-3297.
4. M. Q. Zhang, L. M. Meng, Y. C. Yuan and M. Z. Rong, *Journal of Materials Chemistry*, 2010, **20**, 6030-6038.
5. Y. C. Yuan, X. J. Ye, M. Z. Rong, M. Q. Zhang, G. C. Yang and J. Q. Zhao, *ACS Appl Mater Interfaces*, 2011, **3**, 4487-4495.
6. H. Jin, C. L. Mangun, D. S. Stradley, J. S. Moore, N. R. Sottos and S. R. White, *Polymer*, 2012, **53**, 581-587.
7. J. D. Rule, N. R. Sottos and S. R. White, *Polymer*, 2007, **48**, 3520-3529.
8. B. J. Blaiszik, N. R. Sottos and S. R. White, *Composites Science and Technology*, 2008, **68**, 978-986.
9. E. N. Brown, N. R. Sottos and S. R. White, *Experimental Mechanics*, 2002, **42**, 372-379.
10. A. C. Jackson, J. A. Bartelt, K. Marczewski, N. R. Sottos and P. V. Braun, *Macromolecular Rapid Communications*, 2011, **32**, 82-87.
11. G. Wu, J. An, D. Sun, X. Tang, Y. Xiang and J. Yang, *Journal of Materials Chemistry A*, 2014, **2**, 11614-11620.
12. A. C. Jackson, B. J. Blaiszik, D. McIlroy, N. R. Sottos and P. V. Braun, *Polymer Preprints*, 2008, **49**, 967.
13. S. H. Cho, H. M. Andersson, S. R. White, N. R. Sottos and P. V. Braun, *Advanced Materials*, 2006, **18**, 997-1000.
14. S. H. Cho, S. R. White and P. V. Braun, *Chemistry of Materials*, 2012, **24**, 4209-4214.

15. H. Zhang, P. Wang and J. Yang, *Composites Science and Technology*, 2014, **94**, 23-29.
16. H. Zhang and J. Yang, *Smart Materials and Structures*, 2014, **23**, 065003.
17. H. Zhang and J. Yang, *Smart Materials and Structures*, 2014, **23**, 065004.
18. H. Zhang and J. Yang, *Journal of Materials Chemistry A*, 2013, **1**, 12715-12720.
19. C. M. Dry and N. R. Sottos, presented in part at the North American Conference on Smart Structures and Materials, Virginia, USA, 1993.
20. C. Dry, *Composite Structures*, 1996, **35**, 263-269.
21. M. Motuku, U. Vaidya and G. Janowski, *Smart Materials and Structures*, 1999, **8**, 623.
22. S. Bleay, C. Loader, V. Hawyes, L. Humberstone and P. Curtis, *Composites Part A: Applied Science and Manufacturing*, 2001, **32**, 1767-1776.
23. J. Pang and I. Bond, *Composites Part A: Applied Science and Manufacturing*, 2005, **36**, 183-188.
24. R. Trask, G. Williams and I. Bond, *Journal of The Royal Society Interface*, 2007, **4**, 363-371.
25. J. W. Pang and I. P. Bond, *Composites Science and Technology*, 2005, **65**, 1791-1799.
26. R. Trask and I. Bond, *Smart Materials and Structures*, 2006, **15**, 704.
27. M. L. Zheludkevich, D. G. Shchukin, K. A. Yasakau, H. Möhwald and M. G. S. Ferreira, *Chemistry of Materials*, 2007, **19**, 402-411.
28. M. Hucker, I. Bond, A. Foreman and J. Hudd, *Advanced composites letters*, 1999, **8**, 181-189.
29. K. Toohey, N. Sottos and S. White, *Experimental Mechanics*, 2009, **49**, 707-717.
30. K. S. Toohey, C. J. Hansen, J. A. Lewis, S. R. White and N. R. Sottos, *Advanced Functional Materials*, 2009, **19**, 1399-1405.
31. C. J. Hansen, W. Wu, K. S. Toohey, N. R. Sottos, S. R. White and J. A. Lewis, *Advanced Materials*, 2009, **21**, 4143-4147.
32. K. S. Toohey, N. R. Sottos, J. A. Lewis, J. S. Moore and S. R. White, *Nature materials*, 2007, **6**, 581-585.
33. D. Therriault, R. F. Shepherd, S. R. White and J. A. Lewis, *Advanced Materials*, 2005, **17**, 395-399.
34. A. Bejan, S. Lorente and K.-M. Wang, *Journal of applied physics*, 2006, **100**, 033528.
35. H. Williams, R. Trask and I. Bond, *Smart Materials and Structures*, 2007, **16**, 1198.
36. H. Williams, R. Trask and I. Bond, *Composites Science and Technology*, 2008, **68**, 3171-3177.
37. R. Trask and I. Bond, *Journal of The Royal Society Interface*, 2010, **7**, 921-931.
38. A. P. Esser-Kahn, P. R. Thakre, H. Dong, J. F. Patrick, V. K. Vlasko-Vlasov, N. R. Sottos, J. S. Moore and S. R. White, *Advanced Materials*, 2011, **23**, 3654-3658.
39. S. C. Olugebefola, A. R. Hamilton, D. J. Fairfield, N. R. Sottos and S. R. White, *Soft matter*, 2013, **10**, 544-548.
40. T. J. Sill and H. A. von Recum, *Biomaterials*, 2008, **29**, 1989-2006.
41. A. J. Meinel, O. Germershaus, T. Luhmann, H. P. Merkle and L. Meinel, *European Journal of Pharmaceutics and Biopharmaceutics*, 2012, **81**, 1-13.
42. J. H. Park and P. V. Braun, *Advanced Materials*, 2010, **22**, 496-499.
43. E. N. Brown, *The Journal of Strain Analysis for Engineering Design*, 2011, **46**, 167-186.
44. H. Jin, C. L. Mangun, A. S. Griffin, J. S. Moore, N. R. Sottos and S. R. White, *Advanced Materials*, 2014, **26**, 282-287.